*Traffic 2001; **2:** 746–756*
Munksgaard International Publishers

ISSN 1398-9219

Review

Probing the Machinery of Intracellular Trafficking with the Atomic Force Microscope

Sanjay Kumar[1] and Jan H. Hoh[1,2,*]

[1]Department of Physiology, Johns Hopkins University School of Medicine, Baltimore, MD 21205, USA
[2]Department of Chemical Engineering, Johns Hopkins University, Baltimore, MD 21218, USA
**Corresponding author: Jan H. Hoh, jhoh@jhmi.edu*

Atomic force microscopy has emerged as a powerful tool for characterizing single biological macromolecules, macromolecular assemblies, and whole cells in aqueous buffer, in real time, and at molecular-scale spatial and force resolution. Many of the central elements of intracellular transport are tens to hundreds of nanometers in size and highly dynamic. Thus, atomic force microscopy provides a valuable means of addressing questions of structure and mechanism in intracellular transport. We begin this review of recent efforts to apply atomic force microscopy to problems in intracellular transport by discussing the technical principles behind atomic force microscopy. We then turn to three specific areas in which atomic force microscopy has been applied to problems with direct implications for intracellular trafficking: cytoskeletal structure and dynamics, vesicular transport, and receptor–ligand interactions. In each case, we discuss studies which use both intact cellular elements and reconstituted models. While many technical challenges remain, these studies point to several areas where atomic force microscopy can be used to provide valuable insight into intracellular transport at exquisite spatial and energetic resolution.

Key words: atomic force microscopy, AFM, cell mechanics, cytoskeleton, force measurements, imaging, membrane fusion, receptors, vesicles

Received and accepted for publication 27 July 2001

As cell biology advances into the postgenomic era, increasing attention will be paid to the physical and chemical details of the macromolecular interactions that determine cell physiology. Gaining insight into these interactions will require thorough study of both the structure of macromolecular complexes and the forces that govern their assembly. This need is particularly acute in the area of intracellular trafficking, where macromolecular assemblies such as receptor-ligand complexes, cytoskeletal fibers, and lipid vesicles play a central role, but where our knowledge of molecular biology far outstrips our understanding of the underlying physical chemistry. Clearly, these questions require tools which allow one to probe the structure and physical chemistry of a cell under conditions which are both biologically relevant and easily manipulated. Atomic force microscopy (AFM) is emerging as one such technique. AFM enables imaging and mechanical interrogation of single molecules and macromolecular complexes under near-physiological conditions. Less than two decades after its invention, AFM has begun to contribute to the characterization of systems of biological macromolecules, ranging from single molecules to intact cells.

Here, we review the use of AFM in the study of intracellular trafficking. We begin by briefly discussing the technical aspects of the method, including the components of the instrument, common modes of operation, and how it complements traditional forms of microscopy. We then focus on three central problems in intracellular transport in which there has been particularly intense effort to apply AFM: cytoskeletal structure and dynamics, vesicular transport, and receptor–ligand interactions. While we clearly do not present an exhaustive review of the application of AFM to problems in cell biology, these selected examples should help illustrate some of the insights AFM can provide into the molecular and submolecular details of the machinery of intracellular trafficking.

Principles and Modes of Operation

Instrumentation

The central measurement in atomic force microscopy is the interaction force between a sample surface and a probe (tip) affixed to a weak spring cantilever (Figure 1). These cantilevers are typically microfabricated from silicon or silicon nitride and measure between several microns and hundreds of microns in length. The size of the tip apex, which may range from a few nanometers (carbon nanotube tips) to tens of microns (colloidal particles), places fundamental limits on the imaging resolution and plays a dominant role in determining the tip–sample interaction force. The sample is mounted on a piezoelectric ceramic scanner that enables sample movement in the lateral (x,y) and vertical (z) directions. In some instruments, the cantilever is completely stationary during an AFM experiment; all movement is made by the sample via control of the scanner (Figure 2A). AFM has also been combined with optical microscopy into a single instrument; here, in order to provide an optical path, the cantilever is mounted

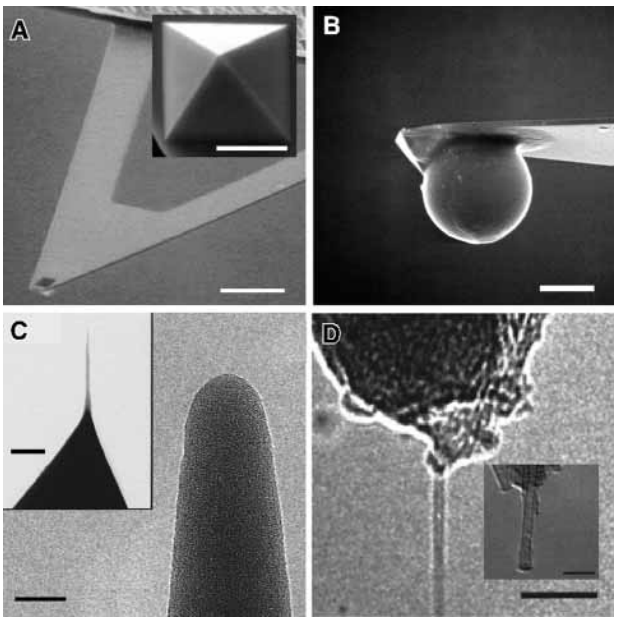

Figure 1: AFM cantilever and tips. (A) Standard pyramidal silicon nitride cantilever (bar is 10 μm), with high-magnification image of tip (inset, bar is 1 μm) (Image courtesy of Eric Henderson). (B) Colloidal particle glued to AFM tip (bar is 5 μm). These tips are widely used for force measurements. (C) Electron-beam deposited (EBD) tip (11) at low magnification (inset, bar is 300 nm) and high magnification (bar is 30 nm) (reprinted with permission, © 2000, American Chemical Society). (D) Carbon nanotube-modified tips of diameter 0.9 nm (main panel) and 2.8 nm (inset) (bar is 10 nm for both) (12) (reprinted with permission, © 2001, American Chemical Society).

on and translated by a piezoelectric scanner while the sample remains stationary (Figure 2B).

Imaging

There are two canonical classes of AFM experiments: imaging and force spectroscopy. The two most commonly used modalities for imaging are contact mode and tapping mode. In contact mode (Figure 3A), the tip is brought into a light but stable contact with the sample, which is then raster-scanned in the x–y plane relative to the cantilever. In this regime, contrast originates from van der Waals repulsion, which dominates the tip–sample interaction force. Topographic variations along the surface lead to deflections of the cantilever; these deflections are monitored by a laser beam which reflects off the back of the cantilever onto a position sensor. Since the cantilever behaves as a linear spring, the deflection is proportional to the interaction force, where the constant of proportionality is the spring constant. Typical spring constants for contact mode AFM cantilevers fall in the range 0.01–1 N/m, allowing the measurement of forces on the order of piconewtons (10^{-12} N). By feeding the signals from this photodiode back to the piezo scanner, the sample's vertical position may be adjusted during the scan so as to maintain a constant deflection (imaging force). Thus, the trace of the piezo's motion is a topographic map of the surface.

In tapping mode (Figure 3B), the cantilever is actively vibrated at around its resonance frequency (typically several kHz to hundreds of kHz) using a piezoelectric actuator. The tip–sample separation distance is set such that the cantilever lightly taps the surface at the lowest point of its oscillation. Here, instead of static deflections, interactions with the sample lead to changes in the amplitude of oscillation of the cantilever. As with contact mode, these changes are measured by a reflected laser beam and fed back to the piezoelectric scanner, which adjusts in z to maintain a constant amplitude. Again, the scanner trace yields the topography of the surface. Because the tip does not maintain constant contact with the surface, tapping mode has also been called 'intermittent contact mode.' There are at least two other important imaging modes in which the cantilever is oscillated. In noncontact (attractive) mode, the tip is vibrated at lower amplitude and senses topography primarily through the influence of noncontact forces that predominate above the sample (1). In magnetic alternating current imaging, the cantilever is magnetically coated and its vibration is driven by an applied, oscillating magnetic field instead of a piezoelectric device (2).

Perhaps the greatest advantage of tapping mode over contact mode is that it minimizes potentially destructive shear and adhesive forces on the sample, a particularly valuable property when imaging cells or biological macromolecules. One disadvantage is that conventional cantilevers tend to have low or poorly defined resonances in aqueous solution, making high-resolution tapping mode imaging a technical challenge. While in principle tapping mode tends to minimize tip–sample interaction forces, in practice, contact mode often provides higher resolution for a given application.

Several other sources of imaging contrast besides topography have been exploited. As a particularly simple example, the error signal (deflection or amplitude) is often useful, particularly in samples in which edges and other topographic gradients are of interest. In tapping mode, the difference in phase of oscillation between the motor driving the cantilever and the cantilever itself may be used as a basis for contrast. These phase differences have been interpreted in terms of energy dissipation by the cantilever and correlated with the viscoelastic properties of the sample (3) and electrostatic interactions between tip and sample (4). In lateral or friction force microscopy (LFM), the torsion of the cantilever is monitored as it scans across the surface, revealing regions of frictional contrast. While we do not review them extensively here, these nontraditional imaging modes are expected to play an increasingly important role in the characterization of biological surfaces by AFM.

Force spectroscopy

In force spectroscopy, the sample is cycled vertically (in z) with respect to the tip while the lateral (x,y) position is fixed. The cantilever deflection is then measured as a function of

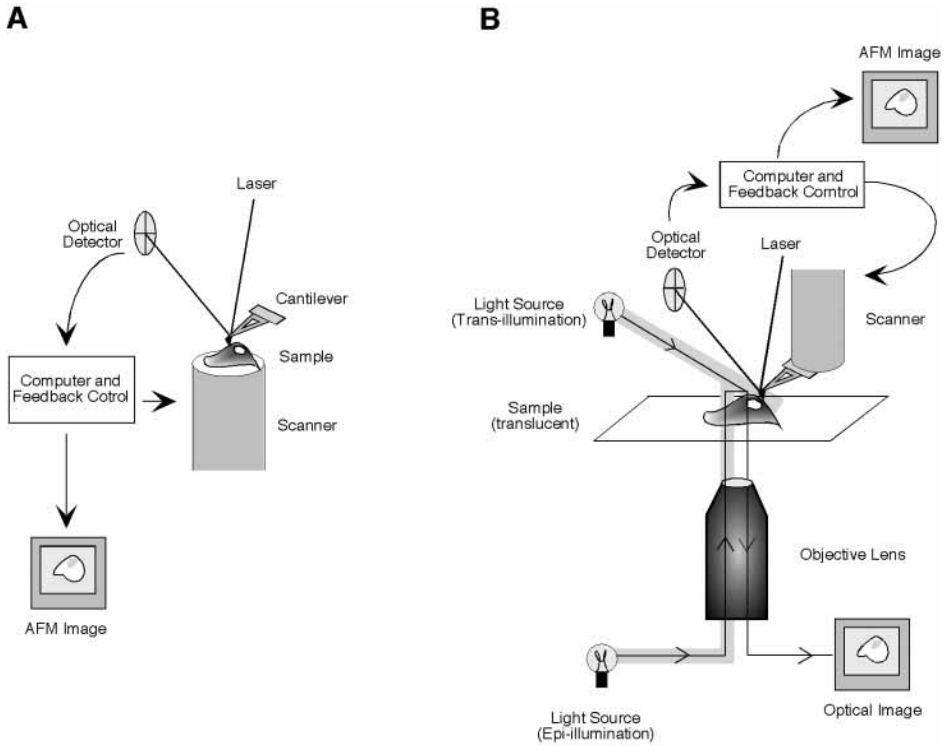

Figure 2: AFM instrumentation. (A) Schematic of stationary-probe AFM. The sample is mounted on a piezoelectric scanner which enables sample manipulation in x, y, and z. The z-position of the cantilever is monitored by a laser beam which reflects onto a position sensor. This position signal is continuously fed back to the scanner, which adjusts to maintain a constant cantilever static deflection (contact mode) or amplitude (tapping mode). The scanner trace thus yields the topography signal. (B) Schematic of a combined AFM/optical microscope. A number of modifications are needed to permit optical access. First, the sample is held stationary and the cantilever is scanned. Second, the sample and substrate must be translucent. Finally, the presence of the scanner in the optical path means that the light source must often be placed out of line with the sample and objective, although this may be overcome by placing a mirrored surface on the scanner (not shown).

piezo scanner (sample) z-position (Figure 4). The data describing deflection vs. sample position, or force curve, may be readily converted to a curve of force vs. tip-sample separation distance which reveals the dominant physical forces between the tip and sample. The portion of the curve in which the probe approaches the sample reveals information about long- and medium-ranged forces such as electrostatic and steric exclusion forces. The portion in which the tip and sample deform one another reflects sample elasticity, and the portion of the curve in which the sample retracts from the tip illustrates tip–sample adhesion and unbinding forces (5). Perhaps most effort in force spectroscopy in biological systems has been directed towards characterizing receptor–ligand interactions, including measurements of binding specificity and strength. Since specific receptor–ligand interactions lie at the heart of virtually all intracellular trafficking and signal transduction pathways, we pay special attention to these studies in this review.

Two emerging areas of force spectroscopy are force mapping and single-molecule stretching. In force mapping, force curves are obtained in an array covering many points on a surface. Each curve is then analyzed to reveal some property of interest, leading to a two-dimensional 'map' of that property (5). In single-molecule stretching experiments, an individual macromolecule is tethered between the tip and surface. As the tip is pulled away from the surface, the macromolecule is stretched and, if it is a protein, unfolded. Each unfolding event produces a characteristic sawtooth-like feature in the force curve, corresponding to unfolding of different domains of the protein. Since the mechanical unfolding of titin was reported in 1997 (6), this method has been applied to many natural and synthetic proteins and extended to polysaccharides (7) and nucleic acids (8). We refer the reader to an excellent review of these experiments (9).

Comparison to other microscopies

The most striking differences between AFM and more traditional types of microscopy lie in three areas: origin and degree of contrast, resolution, and sample preparation. In light and electron microscopy (EM), contrast is based on the ability of a sample to scatter radiation (i.e. a beam of light or electrons). Contrast in AFM originates from forces experienced by the probe as it is scanned across the surface, and may consist of several components (e.g. electrostatics, van der Waals). The degree of contrast is also significantly higher in AFM. While EM has atomic resolution and therefore possesses sufficient power to resolve single biological macro-

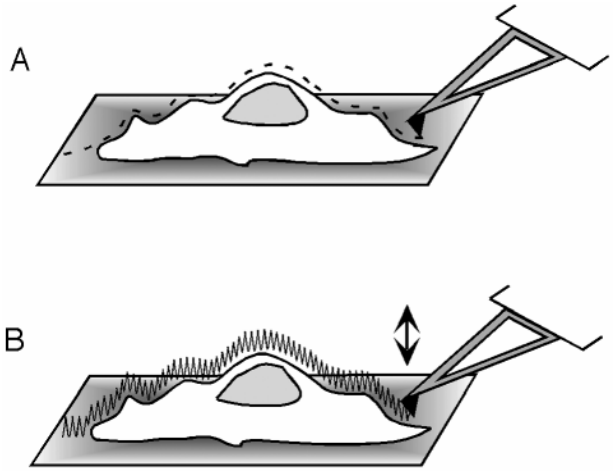

Figure 3: Standard AFM imaging modes. (A) Contact mode imaging. The cantilever is scanned over a sample, and static deflections produce a height signal. (B) Tapping mode imaging. The cantilever is actively vibrated as it scans the sample, and changes in topography produce changes in the amplitude of oscillation.

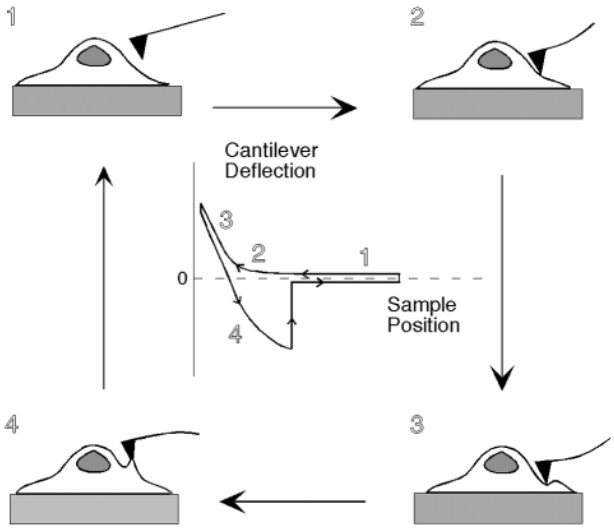

Figure 4: Force curves. 1) At large separation distances, the cantilever and sample do not interact and there is zero deflection. 2) As the sample approaches the tip, the tip deflects; a soft sample (such as a living cell) will likely deform. 3) Further approach leads to greater cantilever deflection and sample deformation. 4) As the tip retracts, the sample adheres to the tip, causing the cantilever to under-deflect. This adhesion results from a complex combination of nonspecific (e.g. electrostatics, van der Waals interactions) and specific (receptor–ligand interactions) forces. When the tip and sample separate, the cycle is completed. Note this schematic illustration of a force curve is rather simplistic. For highly complex samples and tip chemistries, one observes a rich variety of fine structure which results from several superimposed types of tip–sample interaction forces. The approach and retract curves in the noncontact region (1) are slightly separated for clarity.

molecules, contrast is in general poor without the addition of enhancing agents. By comparison, it is routine to image single, unstained protein and nucleic acid molecules by AFM with excellent contrast. Next, because of diffraction effects, the lateral resolution of traditional far-field light microscopy is fundamentally limited to approximately half the wavelength of the imaging radiation. In AFM, images are not produced by diffraction; instead, lateral (x–y) resolution limits are set by the probe size, cantilever z-sensitivity, and sample properties and typically fall within 0.2–50 nm. Vertical (z) resolution limits are instrumental in origin and typically lie around 0.01 nm. Methods have been developed to sharpen tips beyond the abilities of microfabrication. Electron beam deposition may be used to construct tips with end-radii of 5–10 nm (Figure 1C) (10,11). This limit may be pushed even further by affixing a carbon nanotube to the tip (Figure 1D) (12,13). A final distinguishing feature relates to sample preparation. For biological samples, EM typically requires fixation and staining or cryogenic preparation and imaging under vacuum. Conversely, AFM typically requires no staining, and sample preparation is often accomplished simply by physically adsorbing the sample onto a substrate. AFM therefore combines resolution that approaches EM with sample preparation features that more closely resemble light microscopy, with contrast better than both. With a sample chamber that is accessible for buffer exchange over the course of an experiment, these powerful properties allow one to conduct studies in which soluble factors (ions, ATP, regulatory proteins, pharmacological agents) are introduced to the sample and dynamics are monitored in real time.

AFM carries clear limitations relative to traditional microscopies, as well. First, unlike light microscopy, AFM is a surface characterization technique that cannot directly visualize the interior of a cell. Second, even at its fastest, AFM image acquisition is markedly slower than light microscopy. Third, the scanning process can be invasive, and the imaging forces may damage the sample. Finally, the sample must be immobilized onto a surface, and this may either damage the sample or significantly alter its properties. For these and other reasons, instruments that combine AFM with a second imaging modality have become increasingly widely used. Perhaps the best example of this is combined AFM and light microscopy. Using hybrid instruments, this approach has been taken to concurrently visualize intracellular structures with AFM and fluorescence microscopy (14). Some of these studies are discussed in more detail later in the review.

Cytoskeletal Structure and Dynamics

Understanding the structure and function of cytoskeletal polymers is of direct relevance to intracellular transport. First, transport vesicles utilize the cytoskeleton for directional transport, often through kinesin and other motor proteins (15). Second, the cytoskeleton is critical to the maintenance of cell polarity, which in turn supports directional transport of solutes (16). Third, the cytoskeleton is absolutely critical to cell mo-

tility and cytokinesis (17). Given that the substructural features of these cytoskeletal elements are typically on the order of nanometers, and given the interest in correlating cytoskeletal architecture in cells with external mechanical stimuli, the AFM is well suited to address structural and mechanical questions about the cytoskeleton. We first consider studies with isolated cytoskeletal filaments before moving on to studies performed in the context of whole cells.

Purified cytoskeletal filaments

The three major classes of cytoskeletal polymers, actin, microtubules, and intermediate filaments, have all been successfully imaged *in vitro* by AFM. Of these three, microtubules (MTs) have received the most attention in the published literature (Figure 5A). Despite the presence of several established purification protocols, high-resolution imaging of MTs has posed a formidable challenge. Much of this challenge results from difficulty finding substrates and imaging conditions under which the MTs are immobilized but do not significantly deform or rupture, forcing investigators to take creative approaches to substrate and sample preparation. By crosslinking MTs with glutaraldehyde and using glass substrates coated with polylysine, Vater and coworkers were among the first to successfully image MTs in air and solution (18). Later, Vinckier and colleagues induced and arrested MT polymerization at different times and presented AFM images of the resulting structures. These images showed progressive polymerization and growth over 20–30 min; the authors also used force spectroscopy to estimate the elastic moduli of individual microtubules (19). Importantly, both papers recog-

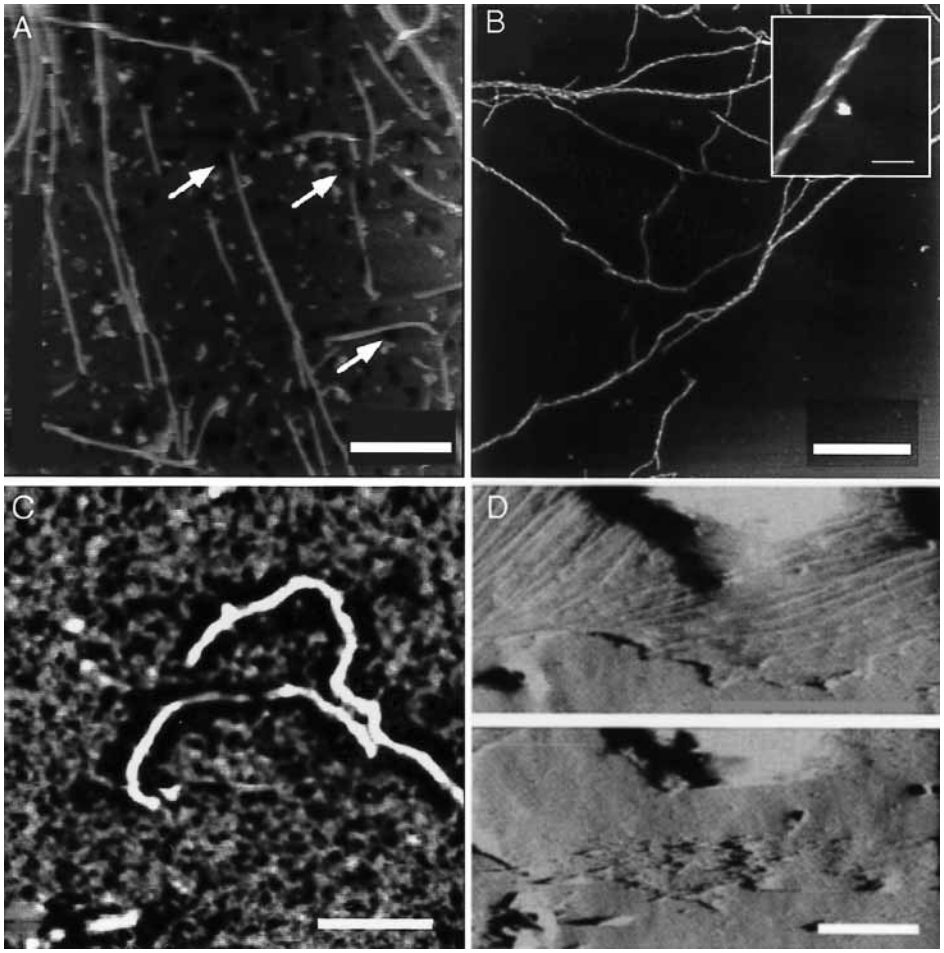

Figure 5: AFM and the cytoskeleton. (A) Microtubules. This image shows microtubules adsorbed to a lipid bilayer in buffer (bar is 2 μm) (20) (reprinted with permission, © 2000 Springer-Verlag, Figure 2A from cited reference). (B) Actin filaments. This image was acquired by cryo-AFM (25). Single filaments associate longitudinally to form rafts which are in turn connected by branching structures (bar is 400 nm). Higher magnification imaging shows the packing of single filaments within rafts (inset, bar is 50 nm) (reproduced with permission, © 2000, Biophysical Society). (C) Intermediate filaments. This image of native neurofilaments (NFs) under buffer shows zones around the filament backbone from which contaminant particles are excluded (bar is 500 nm) (26) (reprinted with permission, © 1997, American Chemical Society). (D) Cytoskeletal imaging *in situ*. In the deflection image of an untreated glial cell (top), a prominent network of filamentous structures is observed in the cytoplasm. When the cell is treated with cytochalasin B, an inhibitor of actin polymerization, this network disappears (bottom) and the cell membrane is rendered labile to repeated scanning (bar is 25 μm) (29) (reproduced with permission, © 1992, American Association for the Advancement of Science).

nized that AFM overestimates microtubule diameters by as much as a factor of four when compared to EM (i.e. 110 nm vs. 25–30 nm). This discrepancy results from the finite size of the tip, which causes apparent broadening of structures that are small relative to the tip. More recent efforts have focused on identifying MT substructures such as protofilaments and attempting to capture MT interactions with accessory motor proteins (20).

Efforts to study actin filaments *in vitro* by AFM have faced similar technical challenges. Several groups have attempted to use AFM to image actin filaments in ambient and aqueous conditions (21–24), although resolution of filament substructure has been limited. Using a custom-built AFM which operates at cryogenic temperatures, Shao and coworkers markedly improved the resolution of individual filaments (Figure 5B) (25). They obtained images of ribbon- and raft-like structures containing several single actin filaments each. The images also clearly show the right-handed helicity of the filaments and a well-defined intrahelical repeat of 35–40 nm, both in excellent agreement with EM. One finding not previously seen by EM was 'branching' junctions in which single filaments formed bridges between two actin rafts. These bridges may help account for the high viscoelasticity of pure, dilute actin gels. Later, Shao et al. presented images of actin paracrystals adsorbed to cationic lipid bilayers (23). This study provided further insight into the packing of actin filaments within rafts, and provides a foundation for AFM characterization of complexes of actin and actin binding proteins.

Intermediate filaments (IF's) are the least well studied of the three types of cytoskeletal fibers by AFM. Neurofilaments (NFs) provide an example of the application of AFM imaging and force spectroscopy to IF's (Figure 5C). NFs are the primary cytoskeletal components of large, myelinated neurons. Through interfilament interactions mediated by their C-terminal 'sidearm' domains, NFs form an ordered intracellular framework which helps maintain neuronal polarity and patency. The structure of the sidearms and thus the origin of interfilament interactions remains controversial. While imaging native NFs purified from bovine spinal cord, Brown and Hoh observed 100–200-nm-wide zones surrounding the backbone of each NF from which contaminants in the preparation were excluded (26). Using direct force measurements, they also found that the NFs generate a long-range repulsive force that persists in the presence of high salt concentration. They interpreted these findings to mean that the sidearm domains are unstructured polypeptides that generate long-range repulsion through thermally driven motion and steric exclusion. This suggests that NFs function by acting as aligned, mutually repulsive, cylindrical 'springs' in the neuron, a hypothesis supported by analysis and simulation of NF distributions from whole neurons (Kumar S, Yin X, Trapp BD, Paulaitis ME, Hoh JH, unpublished data). This approach has also recently been extended to microtubule-associated proteins, which are believed to contribute to microtubule spacing through a similar mechanism (27). AFM has also been used to characterize the structural and mechanical properties of keratin, lending insight into the microstructural origin of the great tensile strength of hair (28).

Cytoskeletal filaments in situ and cell mechanics

The ability of AFM to image samples in aqueous environments and without fixation or staining has been exploited to interrogate living cells and measure changes in cytoskeletal structure and mechanics. The pioneering work of Henderson and colleagues demonstrated that the actin cytoskeleton and subcellular organelles may be imaged without apparent harm to the cell (Figure 5D) (29). The first of these studies used AFM to image a meshlike network in the cell, demonstrating that this was the actin cytoskeleton by correlating it with fluorescence signals from rhodamine-phalloidin stained cells. A later study focused specifically on glial cells, demonstrating that the AFM tip could be used to mechanically manipulate glia and even sever glial processes without killing the cells (30). It also pushed the limits of resolution for subcellular structures, presenting images of the nucleus and mitochondria. Additional studies have examined cytoskeletal dynamics. In one such study (31), the authors used time-lapse imaging to observe extension and withdrawal of lamellipodia, changes in cell shape, and vesicle-like structures traveling along cytoskeletal fibers. Perhaps most strikingly, the authors observed ripple-like cytoskeletal rearrangements propagating both radially outward from the nucleus and around the edge of the cell.

In addition to its importance in trafficking, the cytoskeleton also forms the structural framework which determines cell shape and mechanical properties. Therefore, using AFM to examine cell mechanics can provide insight into cytoskeletal properties. There are many published attempts to use both force curves and spatially resolved force mapping to extract cellular elasticity (32). The recent work of Radmacher and colleagues combines AFM imaging, fluorescence microscopy, and elasticity mapping. Two reports focused on stress fibers and the formation of lamellipodial extensions. The first showed that relative to stably adhered regions of the cell, the active edges of migrating fibroblasts showed greater height fluctuations and higher elasticity with time (33). A more recent study examined the effect of cytoskeletal drugs on cell mechanics. Addition of actin-targeted drugs (cytochalasins B and D and latrunculin A) softened the cell and caused disruption of stress fibers, whereas microtubule targeted drugs (colchicine, colcemide, taxol) produced no morphological or mechanical changes (34). These results illustrate that AFM can be used both to manipulate cells nondestructively and to record cytoskeletal dynamics in real time. Future studies should continue to sharpen spatial and force resolution as well as the biochemical specificity of perturbations and measurements.

Vesicular Transport

The interaction of a transport vesicle with its target membrane is thought to proceed through an orderly series of

events that includes docking, membrane apposition, and ultimately fusion. In many cases, fusion is triggered by discrete events of short time scale such as intracellular calcium release (35). Thus, there is significant interest in learning about vesicle structure at different stages of fusion as well as structural changes induced by soluble effectors. While much valuable insight into the molecular structure of these vesicles has been gained from EM (36), mechanical properties and dynamics are not directly accessible. Here, AFM has yielded new insight, complementing the contributions of established technologies. We again divide AFM studies in this area into two groups: studies with reconstituted systems, and studies with intact biological vesicles.

Reconstituted vesicle systems

Much effort has been devoted to using AFM to study vesicles reconstituted from phospholipids. The underlying paradigm is that reconstituted lipid vesicles serve as well-understood and readily manipulated models of cellular transport vesicles. In one of the first AFM studies of lipid vesicles in buffer, phosphatidylcholine/cholesterol vesicles presenting human IgG were adsorbed onto a gold surface coated with antihuman IgG (37). Contact-mode AFM imaging revealed a heterogeneous surface coated with 80–120-nm-high protrusions interpreted to be individual vesicles. A key finding to emerge from this work was that the lateral resolution of vesicles depends strongly on tip–vesicle contact pressure and lateral shear force, which in turn depends on imaging force and probe dimensions. This complication presents a central technical challenge to AFM imaging of vesicles. In a later study, biotinylated vesicles were adsorbed to an avidin-coated mica surface (38). This study further defined the relationship between imaging forces and observed vesicle morphology and also showed that with increasing vesicle biotinylation, the vesicles may be induced to spread, flatten, and ultimately rupture.

Other studies have focused on characterizing both vesicle substructure and interactions between vesicles. For example, two recent reports presented images of adsorbed, flattened vesicles containing central protrusions. In the first, these structures were detected as transient intermediates in the formation of planar supported bilayers (39). In the second, they were found adsorbed to planar supported bilayers, suggesting that such structures might form during the early stages of vesicle-bilayer fusion (40). The latter study used elasticity mapping to show that the adsorbed vesicles were substantially softer than the underlying bilayer, and also showed the characteristic flat contact interface formed by coadsorbed vesicles, a structural feature previously appreciated only by EM (Figure 6A). Finally, several studies have addressed the mechanism of formation of supported lipid bilayers from the adsorption of small unilamellar vesicles (41–43).

Intact biological vesicles

The properties of biological transport vesicles are less well understood than those of reconstituted vesicles, and the literature of AFM studies of these systems is more limited. Nonetheless, several important strides have been made towards using AFM to characterize these vesicles. In one early report, the authors performed contact mode imaging on cholinergic synaptic vesicles isolated from *Torpedo californica* in air and in buffer (44). In addition to providing valuable proof of principle, this study also showed that one could induce and measure height changes in the vesicles by changing the osmolarity of the solution. Another group performed force spectroscopy and mapping on these vesicles (Figure 6B) (45). Here, the authors showed that the centers of the vesicles were considerably stiffer than their peripheries, and that this center stiffness increases with calcium concentration. EM had already established the presence of 'electron-dense' features at the center of these vesicles, and biochemical studies had established that the centers are proteoglycan-rich. Based on this finding, the authors hypothesized that the calcium binds and cross-links these proteoglycans, producing a stiff, centrally located network.

In addition to simple changes in ionic strength and calcium concentration, vesicular shape changes in response to nucleoside triphosphates have also been studied (46). Here, the authors used zymogen granules (ZGs), secretory vesicles which fuse with the plasma membrane in a GTP-dependent manner. When GTP was added *in situ* to ZGs, the authors observed a 15–25% increase in vesicle height. The authors then hypothesized that the GTP triggers activation of ion channels through heterotrimeric G-proteins.

Receptor–Ligand Interactions

Vesicle docking and fusion *in vivo* require the presence of specific receptor–ligand interactions. Indeed, protein trafficking, antigen processing and presentation, and virtually all other processes of intracellular transport depend on the recognition of ligands by their receptors. The AFM is capable of measuring forces on the piconewton scale, a property that has been exploited to examine receptor–ligand interactions. Molecular recognition is also increasingly being explored as a mechanism of imaging contrast. The vast majority of work in this area has addressed interactions between purified and reconstituted binding partners; an emerging body of literature attempts to extend the application of AFM to measure and characterize these interactions in the context of whole cells.

Pure component receptor-ligand systems

A wide range of receptor-ligand pairs have been studied by AFM. The first studies focused on very high-affinity interactions, particularly that between biotin and avidin (47–49). Typically, streptavidin is anchored to the AFM tip, often by pretreating the tip with biotinylated bovine serum albumin (BSA-biotin). Correspondingly, the substrate is coated with biotin, often as BSA-biotin or by adsorbing biotinylated agarose beads. One then obtains and analyzes force curves. Upon tip–sample approach, the tip and surface bind one another through biotin-avidin recognition. When the tip is re-

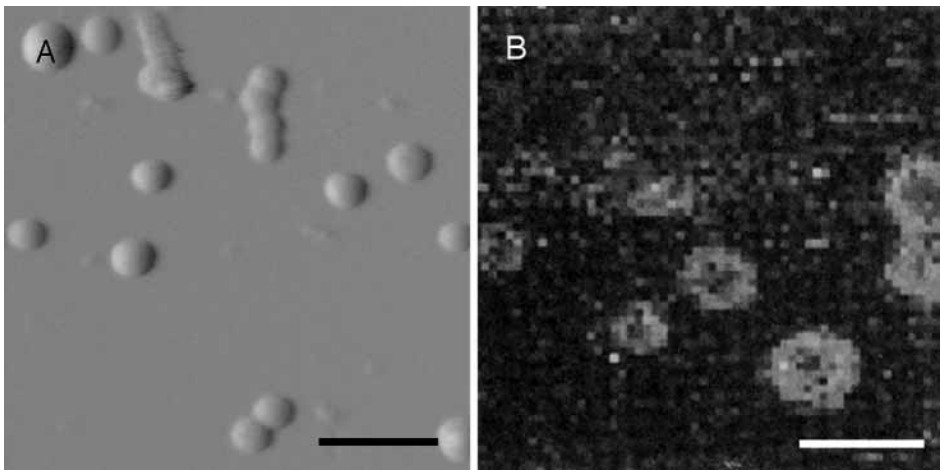

Figure 6: AFM of vesicles. (A) Reconstituted vesicles. This deflection image shows phospholipid-cholesterol vesicles adsorbed to a planar bilayer (40). Where vesicles have coadsorbed, a flat contact interface is seen, characteristic of mutually deformed vesicles (bar is 250 nm) (reprinted with permission, © 2000, American Chemical Society). (B) Cholinergic synaptic vesicles (45). This elasticity map was acquired by taking an array of force curves over the surface, analyzing each curve to obtain the local elastic modulus, and mapping the resulting values (bar is 250 nm). In this map, lighter values correspond to areas of low elasticity (stiffness). Each circular region is a single vesicle; the dark vesicular centers imply that the core is stiffer than the periphery (reproduced with permission, © 1997, Biophysical Society).

tracted, it detaches from the surface in a series of discrete jumps, each corresponding to breakage of one or more biotin-avidin contacts (Figure 7A). Soluble binding inhibitors are often used to demonstrate binding specificity; if the measured adhesion is indeed due to receptor–ligand interactions, addition of an inhibitor to the AFM sample chamber should significantly reduce the binding frequency. The total jump-off force is expected to consist of an integral multiple of the single-pair rupture force. Therefore, by constructing a histogram of rupture forces and determining its period, the single-pair unbinding force may be obtained (50).

As understanding and interpretation of these experiments has improved, attention has shifted away from these model systems to a wide variety of binding partners. Antigen–antibody interactions have served as a particular point of interest. By probing a human serum antigen (HSA)-covered surface with an anti-HSA-functionalized tip, Hinterdorfer and coworkers spatially mapped the location of single surface-bound HSA molecules through adhesion measurements (51). Ros and colleagues used a similar approach to study the effect of point mutations on the binding affinity of fluorescein to the variable region of its cognate antibody (52). Other examples of receptor-ligand pairs under study include ferritin/antiferritin (53), P-selectin/ligand (54) and cadherin/cadherin (55) (Figure 7B). While AFM is clearly a useful tool for detecting the presence of bonds and changes in binding strength, the measured force and energy of bond breakage depend strongly on the rate at which the bond is loaded, as well as a host of other complicating factors (56). Thus, great care must be taken in extracting thermodynamic parameters of bonds from AFM measurements. Willemsen et al. provide an extensive overview of AFM binding studies in which they address such issues and describe many of the other receptor-ligand systems under study (57).

Whole-cell systems

A growing body of research seeks to translate *in vitro* AFM measurements of receptor-ligand binding to systems of whole cells. One of the first of these studies, conducted by Gad et al., sought to map the distribution of polysaccharides on the cell walls of yeast (58). Here, the authors used gold-thiol chemistry to functionalize AFM tips with concavalin A (conA), a lectin which recognizes mannose residues on the yeast cell wall. They then obtained force curves on yeast cells under buffer. While they were unable to spatially resolve the distribution of receptors, they did measure 100–500 pN adhesive forces over cells that could be abolished by adding free mannose. Later work with the conA system showed that chemical cross-linking of the receptors produced marked increases in unbinding forces to an extent that is consistent with cooperative binding (59). Another effort from Lehenkari and Horton (60) took this approach to map integrin distributions on osteoclasts using AFM tips modified with various Arg-Gly-Asp (RGD)-containing peptides. This study showed that RGD-integrin binding depends on a highly specific manner on the peptide context in which the RGD tripeptide is presented, confirming long-standing results from solution assays. A long-term technological goal of receptor-ligand measurements on cells is to develop nondestructive methods for cell identification and sorting. An excellent example of such a study used AFM to type red blood cells (61). The authors probed a mixed monolayer of type-A and O blood cells using a lectin which binds the glycolipids on type-A erythrocytes. Using force mapping, the authors successfully discriminated between the two cell types based on forces of adhesion.

Conclusions and Future Directions

AFM has already demonstrated its utility as a way of acquiring high-resolution images and force measurements of bio-

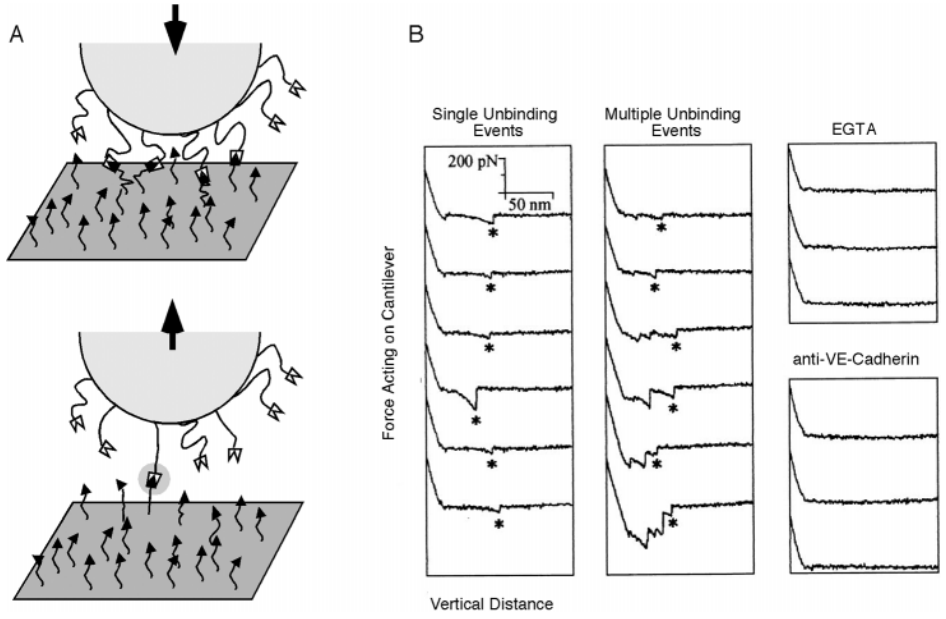

Figure 7: AFM measurements of receptor–ligand interactions. (A) Schematic of typical experiment. A receptor is covalently linked to the AFM probe (shown here as a sphere), often via a flexible linker. Similarly, the cognate ligand is anchored to the substrate. On tip–sample approach (top), several bonds are formed between the two surfaces. On retraction (bottom), each bond is broken in sequence, producing a discrete sawtooth-like deflection of the cantilever. When only one bond is formed, a single sawtooth is observed; when multiple bonds are formed, multiple events are observed, with the final sawtooth corresponding to rupture of the final bond (highlighted). This final deflection provides information about single receptor–ligand interactions. (B) Experimental data for cadherin dimerization. Here, cadherin monomers were adsorbed to the tip and substrate, and many force curves were obtained. The left panel depicts instances in which only one bond formed and ruptured, and the middle panel depicts cases in which multiple bonds formed and ruptured. The asterisks (*) correspond to single pair interactions. The right panel shows that these sawtooth features are attenuated in the presence of EGTA or an anticadherin antibody, implying that these events are specifically due to cadherin–cadherin interactions (55) (Figure reproduced with permission, © 2000 National Academy of Sciences, USA).

logical structures in a near-native environment. In some cases, this rapidly growing body of work has served to verify long-standing results from traditional methods; in others, it has uncovered novel phenomena that provide new insight. This is certainly true in areas relevant to intracellular transport. Here, we have reviewed recent efforts to apply AFM to the study of intracellular trafficking, with a particular focus on cytoskeletal structure and dynamics, vesicular transport, and receptor–ligand interactions. It should be clear that while AFM holds enormous potential to contribute in these areas, much room for improvement remains. First, more effort will likely be devoted to improving the integration of AFM with other techniques, particularly light microscopy. Efforts to combine the power of single molecule fluorescence with single molecule force spectroscopy are particularly exciting. Second, there is ongoing work aimed at developing increasingly versatile and sophisticated tools for the analysis of AFM images and force curves. Third, in terms of improving cantilever performance, much attention continues to be paid to the microfabrication of smaller cantilevers with much higher resonance frequencies (62,63). Much effort has also been put into establishing robust and efficient methods of chemical functionalization of tips. Fourth, improvements in instrumental design are proceeding rapidly. There is a particularly intense focus on developing instruments with faster and more convenient sample transfer and exchange of solutes, with a long-term emphasis on automation. Finally, to fully harness its potential in the biological sciences, more extensive efforts are needed to train life scientists in the theory, practice, and data analysis of AFM. As these areas continue to be addressed, AFM should become more widely used to directly investigate cells and subcellular elements. These efforts will help narrow the gap between our knowledge of the identities of the molecules that drive cell biological phenomena and the physical forces that govern their actions.

Acknowledgments

This work was supported by the U.S. Army (DAMD 17-99-1-9488 to JHH) and the National Institutes of Health (NIH GM64020 to JHH; Medical Scientist Training Program fellowship to SK). We would like to thank our many colleagues for their generosity with their time, suggestions, and data.

References

1. Martin Y, Williams CC, Wickramasinghe HK. Atomic force microscope force mapping and profiling on a sub 100-Å scale. J Appl Phys 1987;61:4723–4729.
2. Raab A, Han WH, Badt D, Smith-Gill SJ, Lindsay SM, Schindler H,

Hinterdorfer P. Antibody recognition imaging by force microscopy. Nat Biotechnol 1999;17:902–905.
3. Cleveland JP, Anczykowski B, Schmid AE, Elings VB. Energy dissipation in tapping-mode atomic force microscopy. Appl Phys Lett 1998;72:2613–2615.
4. Czajkowsky DM, Allen MJ, Elings V, Shao ZF. Direct visualization of surface charge in aqueous solution. Ultramicroscopy 1998;74:1–5.
5. Heinz WF, Hoh JH. Spatially resolved force spectroscopy of biological surfaces using the atomic force microscope. Trends Biotechnol 1999;17:143–150.
6. Rief M, Gautel M, Oesterhelt F, Fernandez JM, Gaub HE. Reversible unfolding of individual titin immunoglobulin domains by AFM. Science 1997;276:1109–1112.
7. Marszalek PE, Pang YP, Li HB, El Yazal J, Oberhauser AF, Fernandez JM. Atomic levers control pyranose ring conformations. Proc Natl Acad Sci USA 1999;96:7894–7898.
8. Clausen-Schaumann H, Rief M, Tolksdorf C, Gaub HE. Mechanical stability of single DNA molecules. Biophys J 2000;78:1997–2007.
9. Fisher TE, Oberhauser AF, Carrion-Vazquez M, Marszalek PE, Fernandez JM. The study of protein mechanics with the atomic force microscope. Trends Biochem Sci 1999;24:379–384.
10. Keller DJ, Chou CC. Imaging steep, high structures by scanning force microscopy with electron-beam deposited tips. Surf Sci 1992;268: 333–339.
11. Skarman B, Wallenberg LR, Jacobsen SN, Helmersson U, Thelander C. Evaluation of intermittent contact mode AFM probes by HREM and using atomically sharp CeO_2 ridges as tip characterizer. Langmuir 2000;16:6267–6277.
12. Hafner JH, Cheung CL, Oosterkamp TH, Lieber CM. High-yield assembly of individual single-walled carbon nanotube tips for scanning probe microscopies. J Phys Chem B 2001;105:743–746.
13. Wong SS, Woolley AT, Odom TW, Huang JL, Kim P, Vezenov DV, Lieber CM. Single-walled carbon nanotube probes for high-resolution nanostructure imaging. Appl Phys Lett 1998;73:3465–3467.
14. Mathur AB, Truskey GA, Reichert WM. Atomic force and total internal reflection fluorescence microscopy for the study of force transmission in endothelial cells. Biophys J 2000;78:1725–1735.
15. Kamal A, Goldstein LSB. Connecting vesicle transport to the cytoskeleton. Curr Opin Cell Biol 2000;12:503–508.
16. Okamoto CT, Forte JG. Vesicular trafficking machinery, the actin cytoskeleton, and H+-K+-ATPase recycling in the gastric parietal cell. J Physiol (Lond) 2001;532:287–296.
17. Schmidt A, Hall MN. Signaling to the actin cytoskeleton. Annu Rev Cell Dev Biol 1998;14:305–338.
18. Vater W, Fritzsche W, Schaper A, Bohm KJ, Unger E, Jovin TM. Scanning force microscopy of microtubules and polymorphic tubulin assemblies in air and in liquid. J Cell Sci 1995;108:1063–1069.
19. Vinckier A, Dumortier C, Engelborghs Y, Hellemans L. Dynamical and mechanical study of immobilized microtubules with atomic force microscopy. J Vac Sci Technol B 1996;14:1427–1431.
20. Kacher CM, Weiss IM, Stuart RJ, Schmidt CF, Hansma PK, Radmacher M, Fritz M. Imaging microtubules and kinesin decorated microtubules using tapping mode atomic force microscopy in fluids. Eur Biophys J Biophys Lett 2000;28:611–620.
21. Buguin A, Du Roure O, Silberzan P. Active atomic force microscopy cantilevers for imaging in liquids. Appl Phys Lett 2001;78:2982–2984.
22. Fritz M, Radmacher M, Cleveland JP, Allersma MW, Stewart RJ, Gieselmann R, Janmey P, Schmidt CF, Hansma PK. Imaging globular and filamentous proteins in physiological buffer solutions with tapping mode atomic force microscopy. Langmuir 1995;11:3529–3535.
23. Shi D, Somlyo AV, Somlyo AP, Shao Z. Visualizing filamentous actin on lipid bilayers by atomic force microscopy in solution. J Microsc 2001;201:377–382.
24. Bustamante C, Erie DA, Keller D. Biochemical and structural applications of scanning force microscopy. Curr Opin Struct Biol 1994;4: 750–760.
25. Shao ZF, Shi D, Somlyo AV. Cryoatomic force microscopy of filamentous actin. Biophys J 2000;78:950–958.
26. Brown HG, Hoh JH. Entropic exclusion by neurofilament sidearms: a mechanism for maintaining interfilament spacing. Biochemistry 1997;36:15035–15040.
27. Mukhopadhyay R, Hoh JH. AFM force measurements on microtubule-associated proteins: the projection domain exerts a long-range repulsive force. FEBS Lett 2001;in press.
28. Parbhu AN, Bryson WG, Lal R. Disulfide bonds in the outer layer of keratin fibers confer higher mechanical rigidity: correlative nano-indentation and elasticity measurement with an AFM. Biochemistry 1999;38:11755–11761.
29. Henderson E, Haydon PG, Sakaguchi DS. Actin filament dynamics in living glial cells imaged by atomic force microscopy. Science 1992;257:1944–1946.
30. Parpura V, Haydon PG, Henderson E. 3-dimensional imaging of living neurons and glia with the atomic force microscope. J Cell Sci 1993;104:427–432.
31. Schoenenberger CA, Hoh JH. Slow cellular-dynamics in MDCK and R5 cells monitored by time-lapse atomic force microscopy. Biophys J 1994;67:929–936.
32. Vinckier A, Semenza G. Measuring elasticity of biological materials by atomic force microscopy. FEBS Lett 1998;430:12–16.
33. Rotsch C, Jacobson K, Radmacher M. Dimensional and mechanical dynamics of active and stable edges in motile fibroblasts investigated by using atomic force microscopy. Proc Natl Acad Sci USA 1999;96: 921–926.
34. Rotsch C, Radmacher M. Drug-induced changes of cytoskeletal structure and mechanics in fibroblasts: an atomic force microscopy study. Biophys J 2000;78:520–535.
35. Brunger AT. Structural insights into the molecular mechanism of calcium-dependent vesicle-membrane fusion. Curr Opin Struct Biol 2001;11:163–173.
36. Mironov AA, Polishchuk RS, Luini A. Visualizing membrane traffic *in vivo* by combined video fluorescence and 3D electron microscopy. Trends Cell Biol 2000;10:349–353.
37. Shibata-Seki T, Masai J, Tagawa T, Sorin T, Kondo S. *In situ* atomic force microscopy study of lipid vesicles adsorbed on a substrate. Thin Solid Films 1996;273:297–303.
38. Pignataro B, Steinem C, Galla HJ, Fuchs H, Janshoff A. Specific adhesion of vesicles monitored by scanning force microscopy and quartz crystal microbalance. Biophys J 2000;78:487–498.
39. Jass J, Tjarnhage T, Puu G. From liposomes to supported, planar bilayer structures on hydrophilic and hydrophobic surfaces: an atomic force microscopy study. Biophys J 2000;79:3153–3163.
40. Kumar S, Hoh JH. Direct visualization of vesicle-bilayer complexes by atomic force microscopy. Langmuir 2000;16:9936–9940.
41. Egawa H, Furusawa K. Liposome adhesion on mica surface studied by atomic force microscopy. Langmuir 1999;15:1660–1666.
42. Muresan AS, Lee KYC. Shape evolution of lipid bilayer patches adsorbed on mica: an atomic force microscopy study. J Phys Chem B 2001;105:852–855.
43. Reviakine I, Brisson A. Formation of supported phospholipid bilayers from unilamellar vesicles investigated by atomic force microscopy. Langmuir 2000;16:1806–1815.
44. Parpura V, Doyle RT, Basarsky TA, Henderson E, Haydon PG. Dynamic imaging of purified individual synaptic vesicles. Neuroimage 1995;2:3–7.
45. Laney DE, Garcia RA, Parsons SM, Hansma HG. Changes in the elastic properties of cholinergic synaptic vesicles as measured by atomic force microscopy. Biophys J 1997;72:806–813.

46. Jena BP, Schneider SW, Geibel JP, Webster P, Oberleithner H, Srithar-an KC. G_i regulation of secretory vesicle swelling examined by atomic force microscopy. Proc Natl Acad Sci USA 1997;94:13317–13322.
47. Florin EL, Moy VT, Gaub HE. Adhesion forces between individual ligand-receptor pairs. Science 1994;264:415–417.
48. Moy VT, Florin EL, Gaub HE. Intermolecular forces and energies between ligands and receptors. Science 1994;266:257–259.
49. Lee GU, Kidwell DA, Colton RJ. Sensing discrete streptavidin biotin interactions with atomic-force microscopy. Langmuir 1994;10:354–357.
50. Hoh JH, Cleveland JP, Prater CB, Revel JP, Hansma PK. Quantized adhesion detected with the atomic force microscope. J Am Chem Soc 1992;114:4917–4918.
51. Hinterdorfer P, Baumgartner W, Gruber HJ, Schilcher K, Schindler H. Detection and localization of individual antibody-antigen recognition events by atomic force microscopy. Proc Natl Acad Sci USA 1996;93:3477–3481.
52. Ros R, Schwesinger F, Anselmetti D, Kubon M, Schafer R, Pluckthun A, Tiefenauer L. Antigen binding forces of individually addressed single-chain Fv antibody molecules. Proc Natl Acad Sci USA 1998;95:7402–7405.
53. Allen S, Chen XY, Davies J, Davies MC, Dawkes AC, Edwards JC, Roberts CJ, Sefton J, Tendler SJB, Williams PM. Detection of antigen-antibody binding events with the atomic force microscope. Biochemistry 1997;36:7457–7463.
54. Fritz J, Katopodis AG, Kolbinger F, Anselmetti D. Force-mediated kinetics of single P-selectin/ligand complexes observed by atomic force microscopy. Proc Natl Acad Sci USA 1998;95:12283–12288.
55. Baumgartner W, Hinterdorfer P, Ness W, Raab A, Vestweber D, Schindler H, Drenckhahn D. Cadherin interaction probed by atomic force microscopy. Proc Natl Acad Sci USA 2000;97:4005–4010.
56. Merkel R, Nassoy P, Leung A, Ritchie K, Evans E. Energy landscapes of receptor-ligand bonds explored with dynamic force spectroscopy. Nature 1999;397:50–53.
57. Willemsen OH, Snel MME, Cambi A, Greve J, De Grooth BG, Figdor CG. Biomolecular interactions measured by atomic force microscopy. Biophys J 2000;79:3267–3281.
58. Gad M, Itoh A, Ikai A. Mapping cell wall polysaccharides of living microbial cells using atomic force microscopy. Cell Biol Int 1997;21:697–706.
59. Chen A, Moy VT. Cross-linking of cell surface receptors enhances cooperativity of molecular adhesion. Biophys J 2000;78:2814–2820.
60. Lehenkari PP, Horton MA. Single integrin molecule adhesion forces in intact cells measured by atomic force microscopy. Biochem Biophys Res Commun 1999;259:645–650.
61. Grandbois M, Dettmann W, Benoit M, Gaub HE. Affinity imaging of red blood cells using an atomic force microscope. J Histochem Cytochem 2000;48:719–724.
62. Walters DA, Cleveland JP, Thomson NH, Hansma PK, Wendman MA, Gurley G, Elings V. Short cantilevers for atomic force microscopy. Rev Sci Instrum 1996;67:3583–3590.
63. Hodges AR, Bussmann KM, Hoh JH. Improved atomic force microscope cantilever performance by ion beam modification. Rev Sci Instrum 2001;in press.